

## Qualitative analysis of a class of Bianchi V imperfect fluid cosmologies

A. A. Coley and K. A. Dunn

Citation: *Journal of Mathematical Physics* **33**, 1772 (1992); doi: 10.1063/1.529654

View online: <http://dx.doi.org/10.1063/1.529654>

View Table of Contents: <http://scitation.aip.org/content/aip/journal/jmp/33/5?ver=pdfcov>

Published by the [AIP Publishing](#)

---

### Articles you may be interested in

[Qualitative analysis of the Navier–Stokes equations for evaporation–condensation problems](#)  
*Phys. Fluids* **8**, 1764 (1996); 10.1063/1.868959

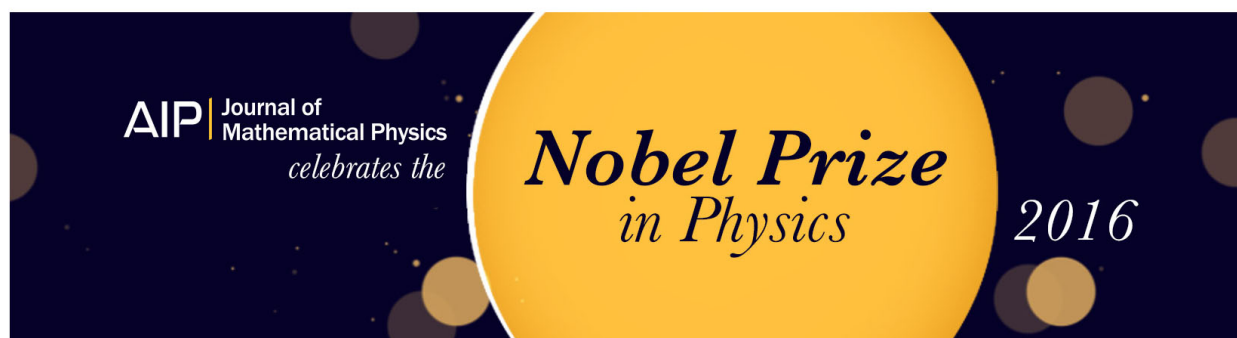
[Qualitative analysis of causal cosmological models](#)  
*J. Math. Phys.* **37**, 2906 (1996); 10.1063/1.531546

[Qualitative analysis of diagonal Bianchi type V imperfect fluid cosmological models](#)  
*J. Math. Phys.* **35**, 4117 (1994); 10.1063/1.530845

[Equations of state and plane-autonomous systems in Bianchi V imperfect fluid cosmology](#)  
*J. Math. Phys.* **31**, 1698 (1990); 10.1063/1.529017

[Global qualitative study of Bianchi universes in the presence of a cosmological constant](#)  
*J. Math. Phys.* **28**, 1658 (1987); 10.1063/1.527473

---



# Qualitative analysis of a class of Bianchi V imperfect fluid cosmologies

A. A. Coley and K. A. Dunn

*Department of Mathematics, Statistics and Computing Science, Dalhousie University, Halifax, Nova Scotia B3H 3J5, Canada*

(Received 12 June 1991; accepted for publication 12 December 1991)

It has been shown that by utilizing a set of “dimensionless” equations of state, the Einstein field equations governing Bianchi V imperfect fluid cosmologies reduce to a plane-autonomous system of equations. This plane-autonomous system shall be investigated here, and the qualitative behavior of the underlying cosmological models shall thereby be obtained.

## I. INTRODUCTION

It is of interest to study cosmological models with a richer structure, both geometrically and physically, than the standard perfect fluid Friedmann–Robertson–Walker (FRW) models. Bianchi V spatially homogeneous models are of particular interest since they are sufficiently complex while being a simple generalization of the negative curvature FRW models. In a recent paper<sup>1</sup> (hereafter referred to as paper I) Bianchi V imperfect fluid cosmologies were investigated. In a second paper<sup>2</sup> (hereafter referred to as paper II), it was shown how the Einstein field equations governing these cosmological models reduce to a plane-autonomous system of equations when a set of “dimensionless” equations of state are utilized, thereby enabling the qualitative nature of the models to be analyzed. It is the aim of the present paper to investigate this plane-autonomous system. A more detailed account of the motivation for this research and the derivation of the various equations can be found in the references of I and II; in particular, for brevity we will adopt the notation that an equation or reference in either of these two papers will be referred to using a label I or II. However, we note that cosmological models that include viscosity have been investigated in an attempt to explain the currently observed highly isotropic matter distribution (II–3) and the high entropy per baryon in the present state of the Universe (I4 and I5), and in order to further study the nature of the initial singularity (I6) and the formation of galaxies (I3). Cosmological models which include heat conduction have also been studied (I7).

We shall utilize the following set of “dimensionless” phenomenological equations of state (see II) for the pressure  $p$ , the bulk viscosity  $\xi$ , and the shear viscosity  $\eta$  in terms of the density  $\rho$  [Eqs. II(3.4)]:

$$p/\theta^2 = p_0 x^l, \quad (1.1a)$$

$$\xi/\theta = \xi_0 x^m, \quad (1.1b)$$

$$\eta/\theta = \eta_0 x^n, \quad (1.1c)$$

where  $p_0$ ,  $\xi_0$ , and  $\eta_0$  are positive constant parameters and

$l$ ,  $m$ , and  $n$  are constants, and where  $x$  is the dimensionless density parameter defined by

$$x = 3\rho/\theta^2. \quad (1.2)$$

We note that  $p/\theta^2$ ,  $\xi/\theta$ , and  $\eta/\theta$  are dimensionless and so Eqs. (1.1) is a set of “dimensionless” equations of state. The motivation for these equations of state has been discussed in detail in Ref. II. Here, we shall simply remark that Eqs. (1.1) ought to be valid (at least) in an asymptotic sense, thereby justifying their use in our qualitative analysis.

Hereafter, we shall assume  $p_0 = \frac{1}{3}(\gamma - 1)$  [ $1 \leq \gamma \leq 2$ ] and  $l = 1$ ; i.e.,  $p$  and  $\rho$  are related by the barotropic equation of state

$$p = (\gamma - 1)\rho; \quad p/\theta^2 = \frac{1}{3}(\gamma - 1)x. \quad (1.1a')$$

We shall also be particularly interested in the case  $m = n = 1/2$ , whence Eqs. (1.1) do not explicitly depend on the expansion  $\theta$ .

Defining the new variable  $\beta$  by

$$\beta = 2\sqrt{3}\sigma/\theta, \quad (1.3)$$

and the new time coordinate  $\Omega$  by

$$\frac{d\Omega}{dt} = -\frac{1}{3}\theta \quad (1.4)$$

(where all quantities not defined here are defined in Refs. I and II) the Einstein field equations [Eqs. I(8c) and (8d); see also Eqs. II(2.12)–(2.14)] for a co-moving LRS Bianchi type-V spatially homogeneous viscous fluid model with heat conduction reduce to the following plane-autonomous system:

$$\frac{d\beta}{d\Omega} = \frac{1}{2}\beta[4 - \beta^2 - (3\gamma - 2)x + 9\xi_0 x^m + 12\eta_0 x^n], \quad (1.5)$$

$$\frac{dx}{d\Omega} = x[(3\gamma - 2)(1 - x) - \beta^2] + \beta\left[2x - 2 + \frac{\beta^2}{2}\right] - 9\xi_0 x^m(1 - x) - 3\eta_0 x^n \beta^2. \quad (1.6)$$

From the “generalized Friedmann equation” [II(2.11)] and the non-negative nature of  $\rho$ , we note that the region of interest is

$$\beta^2 + 4x < 4, \tag{1.7}$$

$$x > 0.$$

Also we note that the field equations imply that there is only one nonzero component of the heat conduction vector. This component,  $q_1$ , satisfies  $q_1 = -\beta\theta$ .

In the next section we shall analyze the plane-autonomous system (1.5) and (1.6) using the techniques employed in Collins<sup>3</sup> and Belinskii and Khalatnikov.<sup>4</sup> The results of the analysis will be discussed in the final sections.

## II. ANALYSIS

The region of interest, defined by (1.7), is the region bounded by the parabola  $\beta^2 + 4x = 4$  and the  $\beta$  axis; we shall denote this region hereafter as  $\mathcal{R}$ . The positive and negative arms of the parabola from (1,0) to (0,2) and (0, -2), respectively, are themselves trajectories.

The first step is to calculate the singular points in  $\mathcal{R}$ , where  $d\beta/d\Omega = 0$  and  $dx/d\Omega = 0$ . From (1.5),  $d\beta/d\Omega = 0$  when  $\beta = 0$  or

$$[4 - \beta^2 - (3\gamma - 2)x] + [9\zeta_0 x^m + 12\eta_0 x^n] = 0; \tag{2.1}$$

but since  $4 - \beta^2 - 4x > 0$  (and  $\gamma < 2$ ) and  $x > 0$  in  $\mathcal{R}$ , this constitutes the sum of two positive definite terms being equal to zero and so each term must be independently zero, viz.,

$$\frac{d\beta}{d\Omega} = 0 \text{ in } \mathcal{R} \Leftrightarrow \beta = 0 \text{ or } (x = 0, \beta = 2)$$

$$\text{or } (x = 0, \beta = -2). \tag{2.2}$$

Utilizing (1.6), we see that, in general, there will be at most five singular points in  $\mathcal{R}$ , namely,

$$(0,0), (0,2), (0, -2), (\Sigma,0), (1,0), \tag{2.3}$$

where  $\Sigma(0 < \Sigma < 1)$  will be defined below.

The analysis then consists primarily of determining the nature of these singular points (and calculating the associated eigendirections). In the case of nondegenerate singular points, this is straightforward (the information is summarized in the figures in the next section). For a degenerate singular point the technique utilized is to change to a polar coordinate system and determine the invariant rays which divide the neighborhood around the singular point into a finite number of sectors (with the singular point as vertex). Each sector is either parabolic

(“fan”), hyperbolic, or elliptic (unless there are no sectors in which case the singular point is a focus or center; this situation does not arise here). In the situation under investigation there are also singular points which are nonanalytic, e.g., in the case  $m = n = 1/2$  (i.e., the equations involve  $\sqrt{x}$ ). These points are analyzed by transforming to a new variable  $u$  and a new time coordinate  $\tau$ , where  $u^2 = x$  and  $d\Omega/d\tau = u$ .

Further information concerning the nature of the trajectories can also be found. Most significantly, we can determine all points in  $\mathcal{R}$  at which  $d\beta/dx = 0$  (i.e., the slope of the trajectory is zero). At such points we must have  $d\beta/d\Omega = 0$ , and we found above [see (2.2)] that in  $\mathcal{R}$  these points consist of all points on the  $x$  axis ( $\beta = 0$ ) and the (singular) points (0,2) and (0, -2). Consequently,  $d\beta/dx$  can only be zero on the  $x$  axis (except at the singular points). Now the  $x$  axis (between the singular points) is itself a trajectory. Thus we have that the  $x$  axis divides  $\mathcal{R}$  into two regions (above and below the  $x$  axis); trajectories cannot cross the  $x$  axis. In these two regions  $d\beta/dx$  is never zero. Therefore, it immediately follows that (i) there exist no closed (periodic) trajectories in  $\mathcal{R}$ , (ii) there exist no singular points that are foci or centers, and (iii) there exist no elliptic sectors at degenerate singular points lying in  $\mathcal{R}$ .

Other useful information is obtained by determining the slope of trajectories crossing the  $\beta$  axis in  $\mathcal{R}$  (e.g., if  $d\beta/dx$  never becomes infinite on  $x = 0$  (i.e.,  $dx/d\Omega \neq 0$ ), then the sign of  $d\beta/dx$  remains the same on the positive and negative branches of the  $\beta$  axis in  $\mathcal{R}$ ), by determining the sign of  $d\beta/dx$  close to the  $x$  axis, and by calculating all points in  $\mathcal{R}$  at which  $dx/d\Omega = 0$  (i.e., at which the slope of the trajectory is infinite).

## III. QUALITATIVE BEHAVIOR OF SOLUTIONS

We shall describe a number of cases and display their phase diagrams in the figures. The specific cases are chosen in order to illuminate the typical behavior, and because they yield all the possible behaviors. We have generally chosen to consider  $m = n$  in each case below; clearly other cases are possible. In addition, we have considered  $m = n = 1/2$  as representative of the case  $0 < m, n < 1$ .

In the figures, arrows refer to evolution in  $\Omega$  – time ( $\Omega \rightarrow +\infty$  indicates  $t \rightarrow 0$ ). Trajectories on the  $x$  axis represent  $k = -1$  FRW cosmological models; M denotes the Milne (flat space-time) model. The label C denotes that the point represents a cigar matter singularity. Figure 1 describes the behavior of the (non-LRS) Bianchi type V cosmologies in the absence of heat conduction and viscosity [see Ref. 3] and are included for purposes of comparison. [In this case the governing equations reduce to a plane-autonomous system for variables  $x$  and  $\beta$  equivalent to Eqs. (1.5) and (1.6), with  $\zeta_0 = \eta_0 = 0$  and

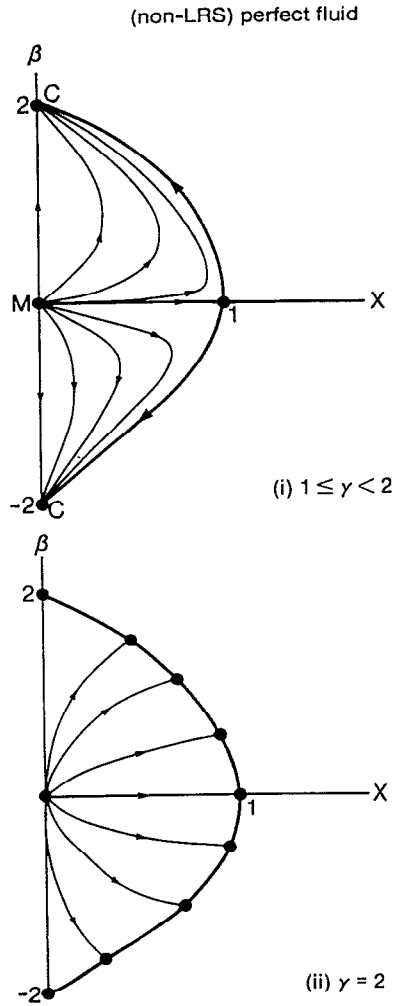


FIG. 1. The behavior of (non-LRS) Bianchi type V cosmologies in the absence of heat conduction and viscosity in terms of the variables  $x$  and  $\beta$  is described (diagrams taken from [3]).

the second term on the right-hand-side of (1.6) omitted and  $\beta$  replaced by  $\bar{\beta}$ ;  $\bar{\beta}$  is defined by  $\bar{\beta} \equiv -(\alpha\beta_1 + \sqrt{3}\beta_2)(3 + \alpha^2)^{-1/2}$ , where  $\alpha$  is a constant and  $\beta_1, \beta_2$  are quantities that measure the rate of shear in terms of the expansion of the (non-LRS) models.] These models isotropize ( $\bar{\beta} \rightarrow 0$  as  $\Omega \rightarrow -\infty$ ) and  $x \rightarrow 0$  as  $\Omega \rightarrow +\infty$ , except for the FRW (point-singularity) models (and for the  $\gamma = 2$  solutions), and so matter is generally dynamically unimportant in the early stages. Cigar singularities occur for  $1 \leq \gamma < 2$ , while for  $\gamma = 2$  barrels or cigars or points are obtained. In the special case  $\gamma = 2$  (i.e., stiff matter), the matter is always dynamically important in that  $x$  is bounded away from zero at all times.

**A.  $\zeta_0 = \eta_0 = 0$**

In this case there is no viscosity, but it does not reduce to the perfect fluid case since the model still contains heat conduction. The phase portraits are given in Fig. 2.

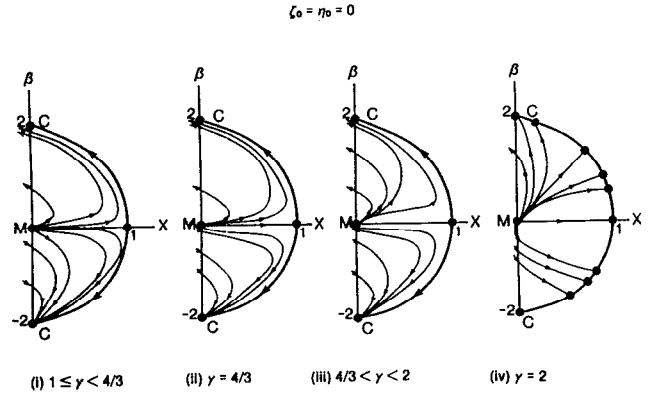


FIG. 2. The evolution of a class of Bianchi V imperfect fluid models in terms of the variables  $x$  and  $\beta$  is described. Arrows refer to evolution in  $\Omega$  time ( $\Omega \rightarrow \infty$  indicates  $t \rightarrow 0$ ). The region of interest is defined by  $x > 0$  and  $\beta^2 + 4x < 4$ . Trajectories on the  $x$  axis represent  $k = -1$  FRW cosmological models: M denotes the Milne (flat space-time) model. The label C denotes that the point represents a cigar matter singularity. In all cases  $p = (\gamma - 1)\rho$ ,  $\zeta/\theta = \zeta_0 x^m$ ,  $\eta/\theta = \eta_0 x^n$  for various choices of the constants  $\gamma, \zeta_0, \eta_0, m$ , and  $n$ . In this figure the case  $\zeta_0 = \eta_0 = 0$  is considered.

For  $\gamma \neq 2$  there are four singular points:  $(1,0)$  is a saddle,  $(0, -2)$  is a stable two-tangent node, and  $(0,0)$  is an unstable two-tangent node (a repelling one-tangent node for  $\gamma = 4/3$ ). The point  $(0,2)$  is a degenerate singular point and will generally be of the complicated node-saddle type. However, we are only interested in the behaviors of the sectors in  $\mathcal{R}$  here, and the (single) sector containing  $\mathcal{R}$  is easily shown to be hyperbolic. Notice that near  $(0,2)$  the system is of the form  $\beta' = -4(\beta - 2) - (3\gamma - 2)x$ ,  $x' = 4(\beta - 2) + (3\gamma - 2)x$ , so that  $\beta' = -x'$  and the solution curves are  $\beta = K - x$  ( $K$  constant). In fact, in all cases the equations near  $(0,2)$  are of the form  $\beta' = -4(\beta - 2) + \alpha x^m$ ,  $x' = 4(\beta - 2) - \alpha x^m$  ( $\alpha$  constant) so that  $(\beta + x)' = 0$ . When  $\gamma = 2$  each point on the boundary  $\beta^2 + 4x = 4$  is a singular point. For this case Eqs. (1.5) and (1.6) can be solved to give the family of solutions  $A\beta^2 - \beta + x = 0$ ,  $\beta \neq 0$ , where  $A$  is an arbitrary constant determined by the initial conditions, and also the solution curve  $\beta = 0$ ,  $0 < x < 1$ .

**B.  $m = n = 0$**

If  $\zeta_0 = 0$ , then there are two singular points:  $(1,0)$  is a saddle and  $(0,0)$  is an unstable two-tangent node (a repelling one-tangent node if  $3\gamma - 4 - 6\eta_0 = 0$ ). In Fig. 3(a) we present the case  $(3\gamma - 4 - 6\eta_0) < 0$ . Near to the origin the phase portraits of the cases  $(3\gamma - 4 - 6\eta_0) = 0$  and  $(3\gamma - 4 - 6\eta_0) > 0$  are similar to those in Figs. 2(ii) and 2(iii), and away from  $(0,0)$  the phase portraits are similar to those in Fig. 3(a). In Fig. 3(a) there is a point  $\beta^*$  on the  $\beta$  axis (with  $-2 < \beta^* < 0$ ) at which  $d\beta/dx$  is infinite. When  $\zeta_0 \neq 0$ , if  $9\zeta_0 < (3\gamma - 2)$ , there are two singular points:  $(1,0)$  is a saddle and  $(\Sigma, 0)$  [with  $\Sigma = 9\zeta_0/(3\gamma - 2)$ ] is an unstable two-tangent node. We

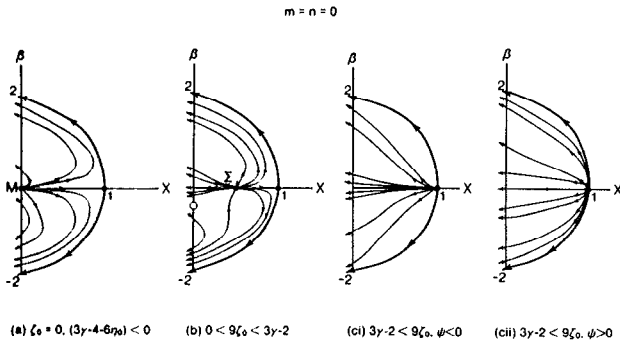


FIG. 3.  $m=n=0$  (see the caption for Fig. 2).

present the phase portraits (Fig. 3b) for the case when  $1 - 2(1 + 3\eta_0)(3\gamma - 2 - 9\xi_0)^{-1} < 0$ . In this case there are two points on the  $\beta$  axis in the interval  $(-2, 0)$  at which  $d\beta/dx$  becomes infinite. When  $9\xi_0 \geq (3\gamma - 2)$ , there is only one singular point. The point  $(1, 0)$  is an unstable two-tangent node [note that when  $9\xi_0 = (3\gamma - 2)$  this point is degenerate]. The phase portraits are presented in Fig. 3(c) (i) and (ii), where  $\psi \equiv 1 - 4(1 + 3\eta_0)(9\xi_0 - (3\gamma - 2))^{-1}$ .

**C.  $m=n=1/2$**

There are degenerate singular points at  $(0, -2)$ ,  $(0, 0)$ , and  $(0, 2)$ . All trajectories in  $\mathcal{R}$  will approach  $(0, -2)$  with the eigendirection associated with the invariant ray  $\theta = \theta^*$ , where  $\tan \theta^* = (9\xi_0 + 12\eta_0)/4$  so that  $0 < \theta^* < \pi/2$ . At  $(0, 0)$  there are invariant rays  $\theta = 0$  and  $\theta = \theta^+$ , where  $\tan \theta^+ = -9\xi_0/2$  so that  $3\pi/2 < \theta^+ < 2\pi$ , which divide  $\mathcal{R}$  up into a number of (or portions of) hyperbolic sectors. At  $(0, 2)$  the (single) sector containing  $\mathcal{R}$  is hyperbolic. There is a fourth singular point  $(1, 0)$ . When  $9\xi_0 < (3\gamma - 2)$  it is a saddle, when  $9\xi_0 > (3\gamma - 2)$ , it is an unstable two-tangent node, and when  $9\xi_0 = (3\gamma - 2)$ , it is degenerate ( $\mathcal{R}$  is part of a parabolic sector). Finally, in the case  $9\xi_0 < (3\gamma - 2)$ , there is a fifth singular point,  $(\Sigma, 0)$  [where  $\Sigma^{1/2} \equiv (9\xi_0)/(3\gamma - 2)$ ], which is an unstable two-tangent node. The phase portrait for the case  $9\xi_0 < (3\gamma - 2)$  is given in Fig. 4(a), while the phase portraits for the case  $9\xi_0 > (3\gamma - 2)$  are given in Fig. 4(b) (i) ( $\psi < 0$ ) and Fig. 4b(ii) ( $\psi > 0$ ). The phase portrait for the case  $9\xi_0 = (3\gamma - 2)$  is given in Fig. 4(c).

**D.  $m=n=1$**

The singular point  $(0, -2)$  is a stable two-tangent node (it is an attracting one-tangent node when  $\lambda \equiv (3\gamma - 2) - 9\xi_0 - 12\eta_0 = -4$ ). The singular point  $(0, 2)$  is degenerate; the (single) sector containing  $\mathcal{R}$  is hyperbolic. In general, there are two further singular points,  $(0, 0)$  and  $(1, 0)$ . When  $9\xi_0 < (3\gamma - 2)$ ,  $(0, 0)$  is an unstable two-tangent node [a repelling one-tangent node if  $(3\gamma - 2) - 9\xi_0 = 2$ ] and  $(1, 0)$  is a saddle. In Fig. 5(a) the phase portraits for the case  $(3\gamma - 2) - 9\xi_0 < 2$ ,  $\lambda > -4$  are presented. When  $9\xi_0 > (3\gamma - 2)$ ,  $(0, 0)$  is a saddle and  $(1, 0)$  is an unstable two-tangent node. The phase diagrams in this case ( $\lambda > -4$ ) are presented in Fig. 5(b) (i) and (ii). Finally, when  $9\xi_0 = 3\gamma - 2$ , each point  $(x, 0)$  for  $0 < x < 1$  is a singular point; i.e., the  $x$  axis is a line-singularity. The phase portrait ( $\lambda > -4$ ) is given in Fig. 5(c). The phase portraits for  $\lambda < -4$  are similar to those given in Fig. 5.

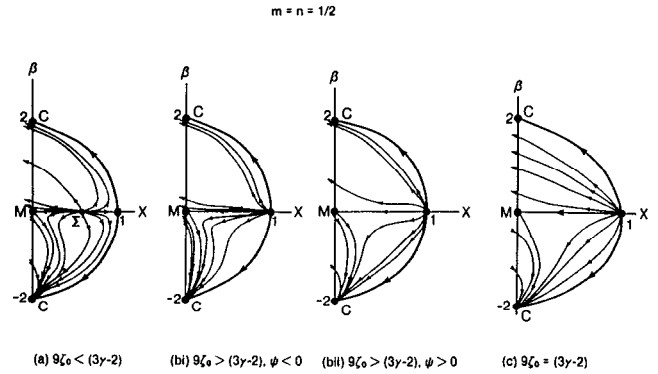


FIG. 4.  $m=n=1/2$  (see the caption for Fig. 2).

**E.  $m > 1, n > 1$**

When  $1 \leq \gamma < 2$ ,  $(0, -2)$  is a stable two-tangent node. [If  $\gamma = 2$ ,  $(0, -2)$  is a degenerate singular point which can be shown to be a node; the phase portraits are similar to those for  $\gamma < 2$ .]  $(0, 2)$  is a degenerate singular point with the (single) sector containing  $\mathcal{R}$  being hyperbolic. The origin  $(0, 0)$  is an unstable two-tangent node (a one-tangent node when  $\gamma = 4/3$ ). If  $9\xi_0 < (3\gamma - 2)$ , the singular point  $(1, 0)$  is a saddle and the phase portraits are given in Fig. 6(a)(i) ( $1 \leq \gamma < 4/3$ ) and 6(a)(ii) ( $4/3 < \gamma < 2$ ). If  $9\xi_0 = 3\gamma - 2$  the singular point  $(1, 0)$  is degenerate, but further analysis shows it to be a saddle. When  $9\xi_0 > (3\gamma - 2)$

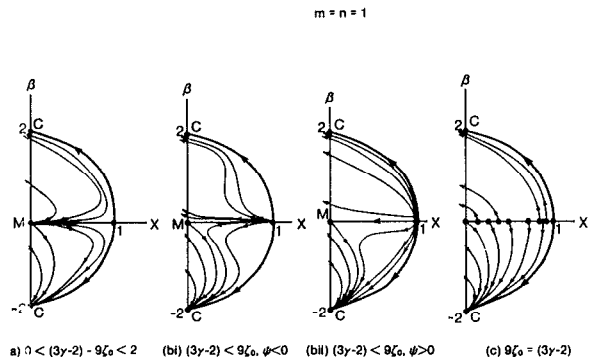


FIG. 5.  $m=n=1$  (see the caption for Fig. 2).

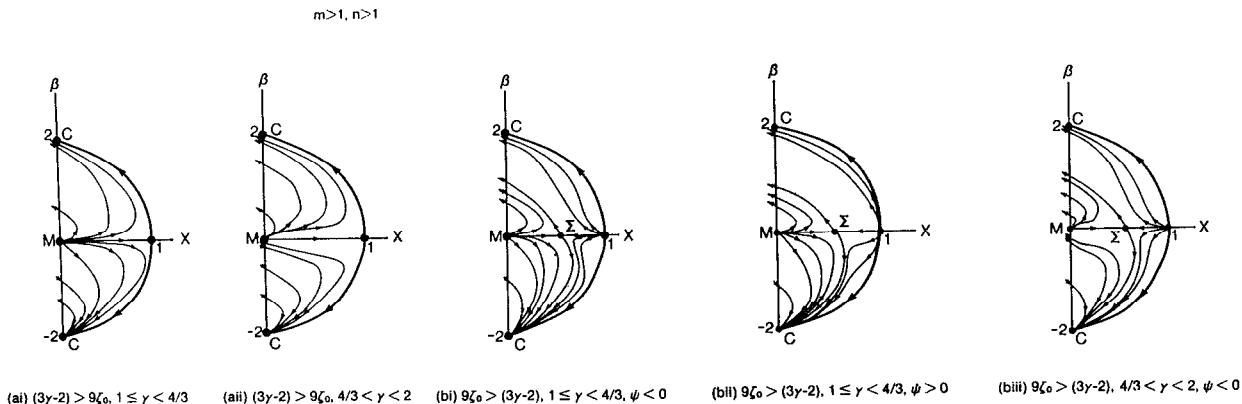


FIG. 6.  $m > 1, n > 1$  (see the caption for Fig. 2).

$-2$ ), the singular point  $(1,0)$  is an unstable two-tangent node and there is also a saddle at  $(\Sigma,0)$  [where  $\Sigma^{m-1} \equiv (3\gamma - 2)/9\xi_0$ ]; the phase diagrams are presented in Fig. 6(b)(i) ( $\psi < 0, 1 \leq \gamma < \frac{4}{3}$ ), 6(b)(ii) ( $\psi > 0, 1 \leq \gamma < \frac{4}{3}$ ), and 6(b)(iii) ( $\psi < 0, \frac{4}{3} < \gamma < 2$ ).

#### IV. DISCUSSION

##### A. Description of the trajectories (Figs. 2–6)

###### 1. $\beta > 0$

All trajectories in the positive  $\beta$  (upper) region of  $\mathcal{R}$  enter  $\mathcal{R}$  at a finite value of  $t$  and can therefore only describe the late (asymptotic) behavior of suitable models. The one exception to this is the case  $\xi_0 = \eta_0 = 0, \gamma = 2$  [Fig. 2(iv)] for which there are solutions which evolve from the boundary  $\beta^2 + 4x = 4$  to the Milne universe at  $(0,0)$ . All these models have  $x$  bounded away from zero at all times and hence matter is dynamically important. These models have no viscosity but do have nonzero heat conduction (compare with Fig. 1(ii)).

###### 2. $\beta = 0$

Trajectories on the  $x$  axis ( $\beta = 0$ ) represent negative curvature FRW models with, at most, bulk viscosity.

When  $\xi_0 = 0$ , the trajectories [Figs. 2 and 3(a)] represent the standard perfect fluid [ $p = (\gamma - 1)\rho$ ] models evolving from the matter-dominated point singularity at  $(1,0)$  to the Milne universe at  $(0,0)$ . In Figs. 5(a) and 6(a)(i) and (ii), where viscosity is present, the evolution is also from the pointlike singularity at  $(1,0)$  to the Milne universe at  $(0,0)$ . These models can be interpreted as perfect fluid FRW cosmologies with density  $\rho$  and pressure  $\bar{p} \equiv p - \xi\theta$  satisfying  $\rho > 0$  and  $\rho + 3\bar{p} > 0$  [since  $(3\gamma - 2) > 9\xi_0$ ].

In the remaining cases that have no singular points on the  $x$  axis, other than  $(0,0)$  and  $(1,0)$ , the evolution is toward  $(1,0)$ . In Fig. 4(b) and (c) and Fig. 5(b) the models start from the Milne universe  $(0,0)$ , at  $t = 0$ , and

expand to the FRW critical point at  $(1,0)$ . In Fig. 3(c) the trajectory on the  $x$  axis enters  $\mathcal{R}$  after a finite time [i.e., there is no singularity of the dynamical system at  $(0,0)$ ] and so we have expansion from the Milne universe  $(0,0)$ , at a finite time  $t > 0$ , to the FRW critical point at  $(1,0)$ . Interpreting these models as perfect fluid FRW cosmologies with density  $\rho$  and pressure  $\bar{p}$ , we have  $\rho + 3\bar{p} < 0$ .

In all other cases there is another singularity on the  $x$  axis at the point  $(\Sigma,0)$  (where  $\Sigma$  is a constant value of  $x, 0 < \Sigma < 1$ , representing a nonzero value of the energy density at this singularity). In all these cases the solution corresponding to the point  $(\Sigma,0)$  can be found exactly. For example, the point  $(\Sigma,0)$  in Fig. 4(a) corresponds to the solution with metric coefficients

$$a(t) = b(t) = (3\gamma - 2)[(3\gamma - 2)^2 - 81\xi_0^2]^{-1/2}t,$$

density

$$\rho(t) = 3(9\xi_0/(3\gamma - 2))^2 t^{-2},$$

pressure

$$p(t) = (\gamma - 1)\rho(t),$$

and bulk viscosity

$$\xi(t) = 27\xi_0^2/(3\gamma - 2)t^{-1}.$$

If this model is interpreted as an FRW perfect fluid cosmology with density  $\rho(t)$  and pressure  $\bar{p} = p - \xi\theta$ , then it is easily seen that  $\rho > 0, \rho + 3\bar{p} = 0$ . The solutions for  $(\Sigma,0)$  in the remaining cases, Figs. 3(b) and 6(b), are of the same form [i.e.,  $a(t) = \alpha t, \alpha = \text{const}, \rho + 3\bar{p} = 0$ ].

In Fig. 3(b) there is a trajectory that represents a universe expanding from the point singularity  $(1,0)$  at  $t = 0$  and approaching the solution  $(\Sigma,0)$  as  $t \rightarrow \infty$ . There is also a trajectory that enters  $\mathcal{R}$  at a finite time  $t_0 > 0$  and

expands to the solution  $(\Sigma, 0)$  at  $t = \infty$ . This solution has the expansion phase consisting of an open FRW solution with bulk viscosity proportional to the expansion  $\theta$ . The trajectories on the  $x$  axis in Fig. 4(a) are exactly the same except that the second trajectory begins at the Milne universe  $(0, 0)$  at  $t = 0$ . In Fig. 6(b), both trajectories expand from the point  $(\Sigma, 0)$  at  $t = 0$  (a pointlike singularity) and asymptotically approach the solutions at  $(1, 0)$  or  $(0, 0)$  as  $t \rightarrow \infty$ .

Finally, in Fig. 5(c), each point  $(x_0, 0)$  on the  $x$  axis ( $0 < x_0 < 1$ ) represents a singular point of the dynamical system. Again, these solutions can be found exactly and are given by

$$a(t) = b(t) = (1 - x_0)^{-1/2}t,$$

$$\rho(t) = 3x_0t^{-2},$$

$$p(t) = 3(\gamma - 1)x_0t^{-2},$$

$$\zeta(t) = ((3\gamma - 2)/3)x_0t^{-1}.$$

As above, they satisfy  $\rho > 0$ ,  $\rho + 3\bar{p} = 0$ . All these solutions represent the endpoint ( $t = \infty$ ) of trajectories that start at the cigar singularity  $(0, -2)$  with zero energy density.

### 3. $\beta < 0$

In the negative  $\beta$  (lower) region of  $\mathcal{R}$  there are a variety of types of trajectories. There are trajectories that evolve from the cigar singularity at  $(0, -2)$  and leave the region  $\mathcal{R}$  after a finite value of  $t$  (Figs. 2, 4, 5, and 6) and therefore only describe the early (asymptotic) behavior of suitable models. There are trajectories which expand from the cigar singularity at  $(0, -2)$  and remain in the region  $\mathcal{R}$  for all time. These models all isotropize as  $t \rightarrow \infty$  and can evolve to the Milne universe at  $(0, 0)$  or to one of the imperfect fluid FRW models at  $(x_0, 0)$ ,  $0 < x_0 < 1$  (see Figs. 2, 4, 5, and 6).

In the case  $m = n = 0$  (Fig. 3) (i.e., viscosity proportional to expansion) all trajectories enter the region  $\mathcal{R}$  at a finite value of  $t > 0$  and can therefore describe the late (asymptotic) behavior of suitable models only.

Finally, the case  $\zeta_0 = \eta_0 = 0$ ,  $\gamma = 2$  [Fig. 2(iv)] has solutions that evolve from the boundary  $\beta^2 + 4x = 4$  ( $\beta < 0$ ), and leave the region at a finite value of  $t$ . Again, these solutions can, at best, describe the early (asymptotic) behavior of suitable models.

A comparison between Fig. 1, which describes the non-LRS perfect fluid Bianchi V trajectories, and Figs. 2–6, which describe the LRS imperfect fluid Bianchi V trajectories, is instructive. All trajectories in the non-LRS perfect fluid case remain in the region where the energy density is non-negative ( $x \geq 0, \beta^2 + 4x \leq 4$ ). The basic picture ( $\gamma \neq 2$ ) is expansion from a cigar singularity at  $(0, 2)$

or  $(0, -2)$ , where the energy density vanishes (and hence matter is not dynamically important), to the Milne universe  $(0, 0)$  as the model isotropizes.

With the introduction of viscosity (and heat conduction), no trajectories remain in the region where the energy density is non-negative for all times ( $0 \leq t < \infty$ ) when  $\beta > 0$ , and many trajectories have this same property in the region  $\beta < 0$ . Those trajectories that do remain in the region ( $x \geq 0, \beta^2 + 4x \leq 4, \beta < 0$ ) also expand from the cigar singularity at  $(0, -2)$  (at  $t = 0$ ) and isotropize asymptotically approaching an FRW model on the  $x$  axis. As above, all of these models evolve from a singularity where the energy-density vanishes.

### B. Energy conditions

As already noted, any trajectory that crosses the  $\beta$  axis must have  $x$ , and thus  $\rho$ , negative after (or before) a finite time. Such models can only be physically realistic asymptotically. All models with  $\beta > 0$  ( $\gamma \neq 2$ ) cross the  $\beta$  axis and consequently cannot be used to construct physically realistic scenarios. The phase portraits are not symmetric about the  $x$  axis due to the second term (odd in  $\beta$ ) on the right-hand side of Eq. (1.6). This term arises due to the nonzero heat conduction. Indeed, as indicated earlier, the nonzero component of the heat conduction vector satisfies  $\beta = -q_1/\theta$  and so a change in sign of  $\beta$  corresponds to a change in the direction of the flow of heat conduction, and the two regions  $\beta > 0$  and  $\beta < 0$  correspond to distinct physics. Henceforward, we shall only consider the case  $\beta < 0$ .

In order to be viable cosmologies it is not sufficient for the models to be confined to the region  $x \geq 0$ . Other energy conditions must be satisfied as well. Therefore, although there are trajectories (for  $\beta < 0$ ) which start and end at singular points and are confined to the region  $\mathcal{R}$  (and so have  $\rho \geq 0$  for all time), the corresponding solutions need not be physically acceptable since the energy conditions may be violated. We can write the energy conditions as follows:

(i) weak energy conditions:

$$-\frac{\lambda_0}{\theta^2} \geq 0, \quad -\frac{\lambda_0}{\theta^2} + \frac{\lambda_\alpha}{\theta^2} \geq 0; \tag{5.1}$$

(ii) dominant energy conditions:

$$-\frac{\lambda_0}{\theta^2} \geq 0, \quad \frac{\lambda_0}{\theta^2} \leq \frac{\lambda_\alpha}{\theta^2} \leq -\frac{\lambda_0}{\theta^2}; \tag{5.2}$$

TABLE I. (For  $\beta < 0$ ) The noted energy conditions are always satisfied if the conditions indicated are satisfied (nr = no restriction).

Energy conditions	$x \approx 0$	$x \neq 0$	
weak	$\zeta_0 - \frac{4}{3}\eta_0 > 0$ $\zeta_0 = \eta_0 = 0$ $\frac{1}{3}\gamma - \zeta_0 + (\frac{4}{3}\eta_0\beta) > 0$ nr	$0 < m, n < 1$ $m = n = 1$ $m, n > 1$	$\zeta_0 - \frac{4}{3}\eta_0 > 0$ $\frac{1}{3}\gamma - \zeta_0 + (\frac{4}{3}\eta_0\beta) > 0 (\forall m, n)$
dominant <sup>a</sup>	$\gamma < 4/3$		$\gamma < 4/3$
strong <sup>a</sup>	$\zeta_0 = \eta_0 = 0$ $\frac{1}{3}(\gamma - 1) - \zeta_0 + (\frac{1}{3}\eta_0\beta) > 0$ nr	$0 < m, n < 1$ $m = n = 1$ $m, n > 1$	$\frac{1}{3}(\gamma - 1) - \zeta_0 + (\frac{1}{3}\eta_0\beta) > 0 (\forall m, n)$

<sup>a</sup>The conditions stated in these cases are those in addition to the weak energy conditions.

(iii) strong energy conditions:

$$-\frac{\lambda_0}{\theta^2} + \sum_{\mu} \frac{\lambda_{\mu}}{\theta^2} \geq 0, \quad -\frac{\lambda_0}{\theta^2} + \frac{\lambda_{\alpha}}{\theta^2} \geq 0 \quad (5.3)$$

( $\alpha = 1, 2, 3$ ), where the eigenvalues of the Bianchi V imperfect fluid energy-momentum tensor are given by

$$\frac{\lambda_0}{\theta^2} = \frac{1}{6}(\gamma - 2)x - \frac{1}{2}\zeta_0 x^m - \frac{1}{3}\eta_0 \beta x^n - \frac{1}{2} \left| \sqrt{\left(\frac{\gamma}{3}x - \zeta_0 x^m - \frac{2}{3}\eta_0 \beta x^n\right)^2 - \Theta^2} \right|, \quad (5.4)$$

$$\frac{\lambda_1}{\theta^2} = \frac{1}{6}(\gamma - 2)x - \frac{1}{2}\zeta_0 x^m - \frac{1}{3}\eta_0 \beta x^n + \frac{1}{2} \left| \sqrt{\left(\frac{\gamma}{3}x - \zeta_0 x^m - \frac{2}{3}\eta_0 \beta x^n\right)^2 - \Theta^2} \right|, \quad (5.5)$$

$$\frac{\lambda_2}{\theta^2} = \frac{\lambda_3}{\theta^2} = \frac{1}{3}(\gamma - 1)x - \zeta_0 x^m + \frac{1}{3}\eta_0 \beta x^n \quad (5.6)$$

[where  $\Theta^2 \equiv (\beta^2/9)(4 - \beta^2 - 4x)$ ].

Now, a given model, with specific values for  $\zeta_0$ ,  $\eta_0$ ,  $m$ ,  $n$ , and  $\gamma$ , may or may not satisfy the weak and/or dominant and strong energy conditions for all  $x$  and  $\beta$ ; in particular, such a model may only satisfy these energy conditions for certain values of  $x$  (if at all), whence the qualitative nature will only be valid asymptotically (e.g., for small  $x$  or  $x \approx 1$ ). Due to the term  $\Theta^2$  in Eqs. (5.4)–(5.6) a full analysis is difficult. Here, we shall simply note that (for  $\beta < 0$ ) the various energy conditions are always satisfied for the parameters indicated in Table I. We also remark that in principle, since all of the eigenvalues (divided by  $\theta^2$ ) are functions of  $x$  and  $\beta$  only, (for particular values of  $\zeta_0$ ,  $\eta_0$ ,  $m$ ,  $n$ , and  $\gamma$ ) the regions in the  $x - \beta$  plane for which the various energy conditions are satisfied can be sketched, thereby providing a simple illustration of which trajectories satisfy the energy conditions.

### C. Previous research

Murphy<sup>5</sup> has given an exactly solvable flat FRW model with bulk viscosity  $\zeta$  proportional to the density, i.e.,  $\zeta = \alpha\rho$ , in which the singularity, in a sense, is eliminated. The “age of the universe” is infinite in this model but the energy conditions are only satisfied after a finite time.

Belinskii and Khalatnikov<sup>4</sup> have studied Bianchi I cosmological models that include viscosity to determine if this characteristic of elimination of the singularity is found in more general models. They assume equations of state  $p = (\gamma - 1)\rho$ ,  $\zeta = \zeta_0\rho^{c_2}$ ,  $\eta = \eta_0\rho^{c_1}$  (at least asymptotically), whence the governing differential equations reduce to a plane-autonomous system. These constants  $c_1$  and  $c_2$  are subject to a number of restrictions, similar to those obtained in the previous section from the energy conditions. A complete picture of the integral curves is then constructed for various suitable values of the exponents and phase portraits are obtained by matching together different asymptotic regions. They arrive at four basic conclusions. First, the cosmological singularity remains an inevitable factor of the evolution of the universe. Second, there are a variety of possible expansion scenarios but near the cosmological singularity the picture is unique—the singularity has infinite curvature invariants but the energy density vanishes at the singularity. Third, there are solutions corresponding to both expansion and contraction of the universe and these differ insofar as the behavior of the energy density of matter near the cosmological singularity is concerned. A contraction starts with isotropic FRW stages and ends with an isotropic FRW singularity. Finally, the process of expansion of the universe will, in general, lead to an isotropic FRW expansion. Depending on the initial conditions, the models evolve to either a node corresponding to a usual FRW picture with a negligible role of viscosity or a node where the viscosity continues to exert a substantial influence.

The situation has been generalized to Bianchi II cosmologies with viscosity by Parnovskii,<sup>6</sup> in which the general conclusions drawn by Belinskii and Khalatnikov are



confirmed. The author also argues that models of Bianchi types VI, VII, VIII, and IX can be considered, but that the picture they give hardly differs qualitatively from the systems already investigated (and, in addition, the resulting systems of equations require the introduction of multidimensional phase spaces and are thus difficult to analyze).

In some related work Belinskii and Khalatnikov<sup>7</sup> have qualitatively studied the effect of the inclusion of bulk viscosity in the standard FRW cosmologies. By determining the behavior of the integral curves when the viscosity asymptotically has the form of a power law in the energy density (i.e., as  $\rho \rightarrow 0$  and  $\rho \rightarrow \infty$ ) and joining them up in these asymptotic regions, ("matched-up") phase portraits are obtained describing models valid for all time. This work has been generalized to include a nonzero cosmological constant.<sup>8</sup> The qualitative nature of isotropic FRW models with bulk viscosity of the form  $\zeta = \zeta_0 \rho^c$  has also been studied in Ref. 9. In particular, models with  $c = \frac{1}{2}$  received special attention, and it was found that the only possible solutions that are structurally stable are those with  $c = \frac{1}{2}$  ( $0 < c < \frac{1}{2}$  if a nonzero cosmological constant is included).

## V. CONCLUSION

By using the equations in Sec. I (derived in Refs. I and II), we have obtained qualitative information about LRS Bianchi type V models containing a viscous fluid and heat conduction with equations of state (1.1). From this we are able to calculate the asymptotic behavior of models to the past and to the future. In particular, we have shown that the general results obtained by Murphy and Belinskii and Khalatnikov hold in the Bianchi V case as well. As found by Murphy,<sup>5</sup> there are open FRW models with viscosity for which there is no initial singularity (cf. Fig. 3); however, the energy conditions will be violated at a finite time in the past in these models. The main conclusions found by Belinskii and Khalatnikov<sup>4</sup> carry over here also. In all cases the models expand as  $t \rightarrow \infty$  (there are no models which contract here) toward an isotropic FRW model. In the non-FRW cases the cosmological singularity remains an inevitable factor of the evolution and the energy density vanishes at the singularity [i.e., at the point  $(0, -2)$ ]. Several FRW models [cf. Figs. 4(b) and (c) and 5(b)] evolve from the nonsingular Milne universe [at  $(0,0)$ ], but the energy density still vanishes at this initial point. We recall that Belinskii and Khalatnikov conclude that "this phenomenon can be interpreted as production of matter by the gravitational field at the instant of the big bang." Again, depending on the situation considered, we can have a negligible role of viscosity asymptotically (at the point  $x = 0, \beta = 0$ ) or the viscosity can continue to exert a substantial influence [at the points  $(x_0, 0), 0 < x_0 < 1$ ]. We find that the global behavior (e.g., types of singular points) depends prima-

rily on the bulk viscosity although the precise (local) details depend on both bulk and shear viscosity.

It may be worth pointing out the differences and similarities between this and previous work. In this work we employ the variables  $x$  and  $\beta$  used by Collins,<sup>3</sup> and generalize his work in the case of a Bianchi V space-time to include dissipative terms. The work by Belinskii and Khalatnikov includes viscous terms; the differences here are that (i) we use variables  $x$  and  $\beta$  (not  $\rho$  and  $H$ ), (ii) heat conduction is also included, and (iii) we employ equations of state  $\zeta/\theta = \zeta_0(\rho/\theta^2)^m$  and  $\eta/\theta = \eta_0(\rho/\theta^2)^n$  (rather than  $\zeta = \zeta_0 \rho^{c_2}$  and  $\eta = \eta_0 \rho^{c_1}$ ). We note that in the particular case  $m = n = 1/2$  ( $c_1 = c_2 = 1/2$ ), these sets of equations of state are the same (although our models are still different since there is nonzero heat conduction). This is the particular case in which our equations of state are independent of the expansion. It is interesting to note that this case has received a lot of attention in the literature.<sup>9</sup>

It has been the aim of this research to study the qualitative nature of cosmological models more complex than those studied so far in the literature. Although the models investigated here are very specialized, this work is at least a first step in the right direction. Obviously, it would be useful to obtain qualitative descriptions, like those in Sec. III, for more general universe models. In situations in which the differential equations describing a cosmology can be reduced to a plane-autonomous system, it is possible to give such a qualitative description; consequently, it is of interest to study these highly specialized situations. While such cosmologies may not exhibit the same behavior as general models, they do, as Collins and Ellis<sup>10</sup> have pointed out, show exact behavior of solutions of the full field equations. As seen above in the case of a class of Bianchi V imperfect fluid models, this behavior is much richer than in many of the cosmologies studied previously.

## ACKNOWLEDGMENT

This research was supported, in part, by the Natural Sciences and Engineering Research Council of Canada through operating grants to each author.

<sup>1</sup>A. A. Coley, *Gen. Rel. Grav.* **22**, 3 (1990).

<sup>2</sup>A. A. Coley, *J. Math. Phys.* **31**, 1698 (1990).

<sup>3</sup>C. B. Collins, *Comm. Math. Phys.* **23**, 137 (1971); *Comm. Math. Phys.* **39**, 131 (1974).

<sup>4</sup>V. A. Belinskii and I. M. Khalatnikov, *Sov. Phys.-JETP* **42**, 205 (1976).

<sup>5</sup>G. L. Murphy, *Phys. Rev. D* **8**, 4231 (1973).

<sup>6</sup>S. L. Parnovskii, *Sov. Phys.-JETP* **45**, 423 (1977).

<sup>7</sup>V. A. Belinskii and I. M. Khalatnikov, *Sov. Phys.-JETP* **45**, 1 (1977).

<sup>8</sup>E. S. Nikomarov and I. M. Khalatnikov, *Sov. Phys.-JETP* **48**, 592 (1978).

<sup>9</sup>Z. Golda, M. Heller, and M. Szydlowski, *Astrophys. Sp. Sci.* **90**, 313 (1983); A. Woszczyna and W. Betkowskii, *Astrophys. Sp. Sci.* **82**, 489 (1982).

<sup>10</sup>C. B. Collins and G. F. R. Ellis, *Phys. Rep.* **56**, 65 (1979).